European Journal of Medicinal Chemistry 148 (2018) 465–476

Contents lists available at ScienceDirect

European Journal of Medicinal Chemistry

journal homepage: http://www.elsevier.com/locate/ejmech

Research paper

# Discovery of carbazole carboxamides as novel RORγt inverse agonists

Yafei Huang, Mingcheng Yu, Nannan Sun, Ting Tang, Fazhi Yu, Xiaoxia Song, Qiong Xie*, Wei Fu, Liming Shao, Yonghui Wang**

*Department of Medicinal Chemistry, School of Pharmacy, Fudan University, 826 Zhangheng Road, Shanghai 201203, China*

ARTICLE INFO

*Article history:*
Received 21 December 2017
Received in revised form
29 January 2018
Accepted 14 February 2018
Available online 16 February 2018

*Keywords:*
Carbazole carboxamides
RORγt inverse agonists
Th17 cells
Autoimmune diseases
Binding mode

ABSTRACT

A novel series of carbazole carboxamides was discovered as potent RORγt inverse agonists using a scaffold hybridization strategy. Structure-activity relationship exploration on the amide linker, carbazole ring and arylsulfone moiety of the hybrid amide **3a** led to identification of potent RORγt inverse agonists. Compound **6c** was found to have a good RORγt activity with an $IC_{50}$ of 58.5 nM in FRET assay, and reasonable inhibitory activity in mouse Th17 cell differentiation assay (58.8% inhibition at 0.3 μM). The binding mode of carbazole carboxamides in RORγt ligand binding domain was discussed.



## 1. Introduction

Th17 cells, a lineage of $CD4^+$ effector T cells characterized by the production of IL-17A and IL-17F, are pathogenic in autoimmune diseases such as multiple sclerosis and psoriasis [1–4]. The retinoic acid receptor-related orphan receptor-gamma-t (RORγt) is a key nuclear receptor of the ROR family that has been implicated in the differentiation and function of Th17 cells [5,6]. Therefore, RORγt inhibitors have potential utility in reducing the activity of Th17 cells and can be developed as therapeutic agents for the treatment of Th17-mediated autoimmune diseases [7–14].

Started with digoxin [15], SR1001 [16] and ursolic acid [17], a few small molecule RORγt inhibitors have been reported in the literature [18–21]. Previously, we reported the discovery of several *N*-aryl amides such as thiazole/thiophene ketone amides [22], thiazole ether amides [23], indole amides [24] and biaryl amides [25,26] as RORγt inverse agonists (Fig. 1). Biaryl amide **1** (or GSK805) exhibited excellent RORγt activity ($IC_{50}$ = 34.0 nM in our FRET assay), strong inhibition of Th17 cell differentiation, good oral bioavailability and CNS penetration, and remarkable efficacy in mouse experimental autoimmune encephalomyelitis (EAE) model, and was therefore employed as a unique tool compound for both *in vitro* and *in vivo* biological and immunological studies [10,27]. However, compound **1** showed some developability issues which prevented it to be further progressed as a clinical candidate. The developability issues could be associated with the compound **1**'s high molecular weight (MW = 532) and high hydrophobicity (cLogP = 5.23), mainly attributed to its biaryl moiety [28]. Thus, one of our lead optimization goals for the *N*-aryl amide series is to identify novel structural moieties to improve compounds' developability profiles.

Recently, Takeda Pharmaceutical Company disclosed in a PCT patent a series of carbazole-containing compounds as RORγt inhibitors [29]. The representative compound **2** (example 14 in Takeda's patent) showed good RORγt activity ($IC_{50}$ = 50.6 nM in our FRET assay). However, the compound **2** has much higher cLogP (6.44) although MW is reasonable (473). Structural superimposition of compounds **1** with **2** in RORγt ligand binding domain (LBD) indicated that both carbazole and biaryl moieties occupied the same hydrophobic pocket of the RORγt LBD (Fig. 2a) [24]. Stimulated by the docking results along with relatively lower MW and cLogP of carbazole structural moiety, we had a hypothesis that replacing the biaryl moiety in **1** with the carbazole moiety in **2**, resulting in hybrid compounds such as **3a**, could reduce MW and cLogP of the amides (**3a**: MW = 421, cLogP = 4.16) while possibly maintaining the RORγt activity based on overlay results of **3a** with **1** (Figs. 2b and 3). To test this hypothesis, we prepared the hybrid

* Corresponding author.
** Corresponding author.
*E-mail addresses:* qxie@fudan.edu.cn (Q. Xie), yonghuiwang@fudan.edu.cn (Y. Wang).

https://doi.org/10.1016/j.ejmech.2018.02.050
0223-5234/

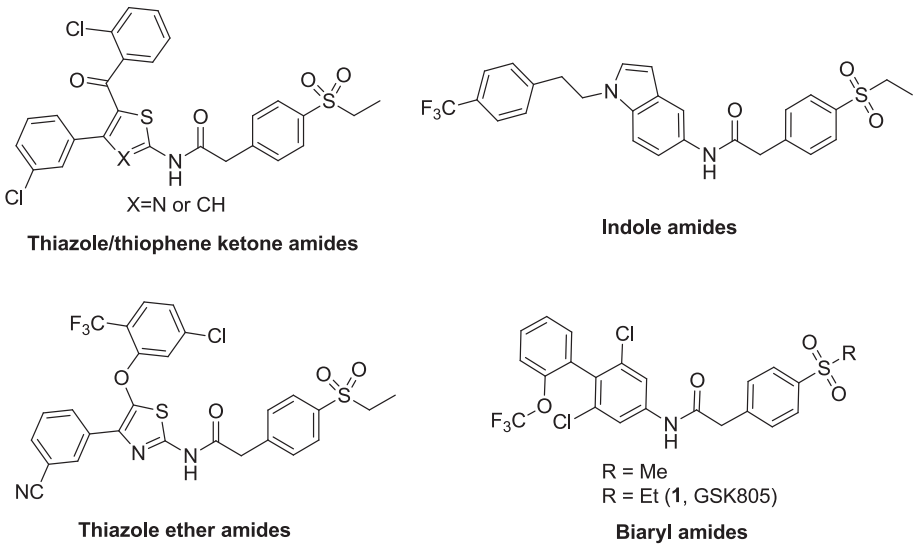


**Fig. 1.** *N*-Aryl amide-based RORγt inverse agonists.

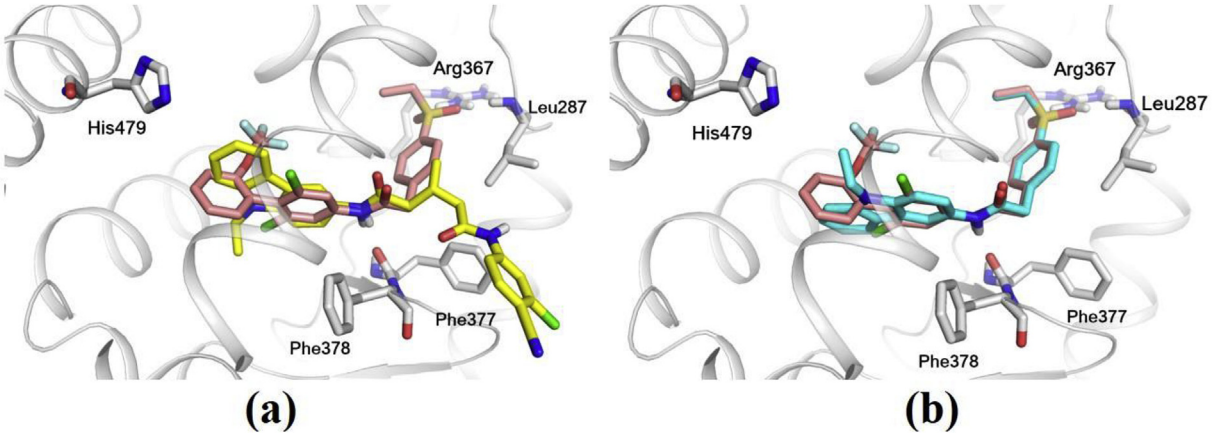


**Fig. 2.** (a) Structural superimposition of the docked poses of **1** (salmon stick) with **2** (yellow stick) in RORγt LBD; (b) Structural superimposition of the docked poses of **1** (salmon stick) with **3a** (cyan stick) in RORγt LBD (PDB: 4NIE). (For interpretation of the references to colour in this figure legend, the reader is referred to the Web version of this article.)

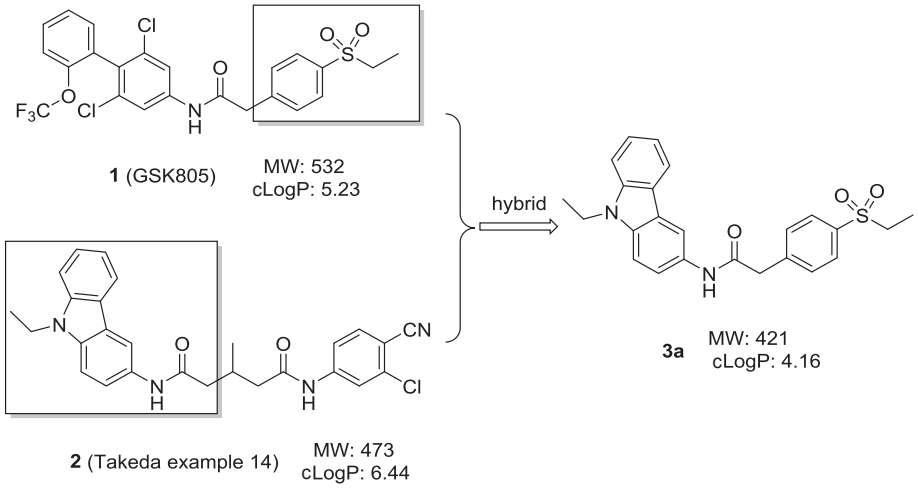


**Fig. 3.** Hybridization strategy for the design of novel RORγt inhibitors.

compound **3a** and tested it in the RORγ FRET assay. To our delight, the hybrid carbazole amide compound **3a** showed a decent RORγt activity with an $IC_{50}$ of 170 nM and could be employed as new chemical starting point for further optimization. In this paper, we reported the design, synthesis, structure-activity relationship (SAR) and binding mode studies of a series of carbazole-containing compounds as novel RORγt inhibitors.

## 2. Result and discussion

### 2.1. Compound design

Since Takeda's compounds such as **2** have "longer" linker between the left-hand side (LHS) carbazole moiety and the right-hand side (RHS) aryl moiety than that in the biaryl amides such as **1**, we first designed a few compounds (**3a-3e**) with different linkers, trying to identify a suitable one to connect the LHS carbazole moiety and RHS arylsulfone moiety. Then, with the best linker (-$CONHCH_2$-) identified, we designed some new compounds (**4a-4d**, **5a-5h**, **6a-6d, 7a-7d**) with the LHS carbazole moiety and RHS arylsulfone moiety modified, respectively, trying to optimize the carboxamides for better RORγt activity (Fig. 4).

### 2.2. Chemistry

A versatile synthesis of the general structures of carbazole carboxamides was developed and outlined in Scheme 1. The synthesis started with Buchwald-Hartwig cross coupling of amines and halides to form diphenylamines **8** or **9**, which could be converted to carbazoles **10** through cyclization. To introduce different *N*-substituents at the carbazolyl moiety, various bromides or iodides were reacted with **10** under alkaline condition to yield **11**, which produced carbazolyl carboxylic acids **12** upon hydrolysis. Condensation of **12** with amines **14** obtained from reduction of cyanides **13** afforded the desired carbazolyl amides (**3b**, **5a-5h**, **6a-6d**, **7a-7d**).

Reagents and conditions: ($a_1$) $Pd(OAc)_2$, rac-BINAP, $K_2CO_3$, toluene; ($a_2$) $Pd(OAc)_2$, rac-BINAP, $Cs_2CO_3$, toluene; ($b_1$) $Pd(OAc)_2$, HOAc, 130 °C; ($b_2$) $PdCl_2(PPh_3)_2$, $NaOAc{\cdot}3H_2O$, DMF, microwave; (c) NaH; (d) KOH, EtOH/$H_2O$, 100 °C; (e) Raney Ni, $H_2$, MeOH, rt; (f) HATU, DIEA, DCM, rt.

For the non-carbazolyl carboxamides analogues (**4a-4d**) (Scheme 2), the synthesis started with Fischer indole synthesis from 4-hydrazinylbenzoic acid and ketones to form indole-5-carboxylic acids **15**, which were protected as esters **16**, then converted to **17** upon ethylation with ethyl iodide. Condensation of **18**, the hydrolysis product of **17**, with amine **14a** afforded compounds **4a-4d**.

Reagents and conditions: (a) HCl, 1,4-dioxane, reflux; (b) MeOH, $H_2SO_4$; (c) NaH, EtI, DMF, 0°C-rt; (d) LiOH, EtOH/$H_2O$, rt; (e) HATU, DIEA, DCM, rt.

Synthetic procedures of **3a-3e** were described in the supporting information.

### 2.3. Structure-activity relationship

Firstly, a few compounds with different linkers between carbazole and arylsulfone moieties were designed, synthesized and evaluated in the RORγ FRET assay (Table 1). Compound **3b** with a reversed amide linker relative to **3a** showed essentially the same RORγt activity. Overlay of **3a** and **3b** in RORγt LBD revealed that the two compounds aligned to each other very well, maintaining the same key hydrogen bonding interactions with the receptor (Fig. 5). Replacing the amide linker in **3a** with a urea linker (**3c**) dropped the RORγt activity dramatically. Extending the length of the linker by adding polar amide groups further lowered the activity (**3d**) or completely aborted the activity (**3e**) although cLogPs of **3d** and **3e**

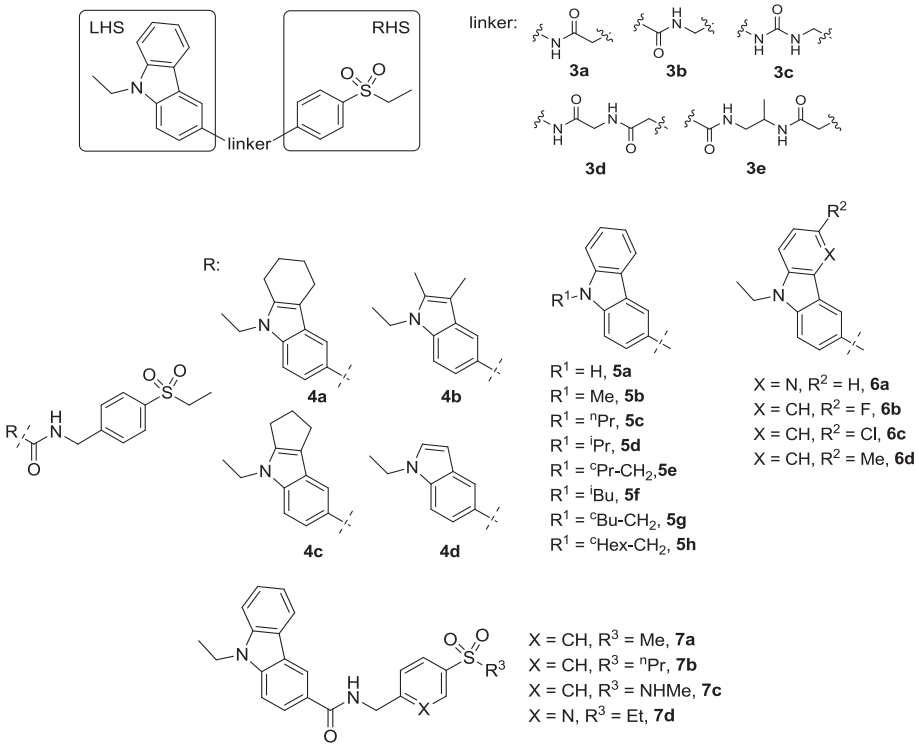


**Fig. 4.** Target compounds with amide linker (**3a-e**), carbazole ring (**4a-d, 5a-h, 6a-d**) and arylsulfone moiety (**7a-d**) modified.

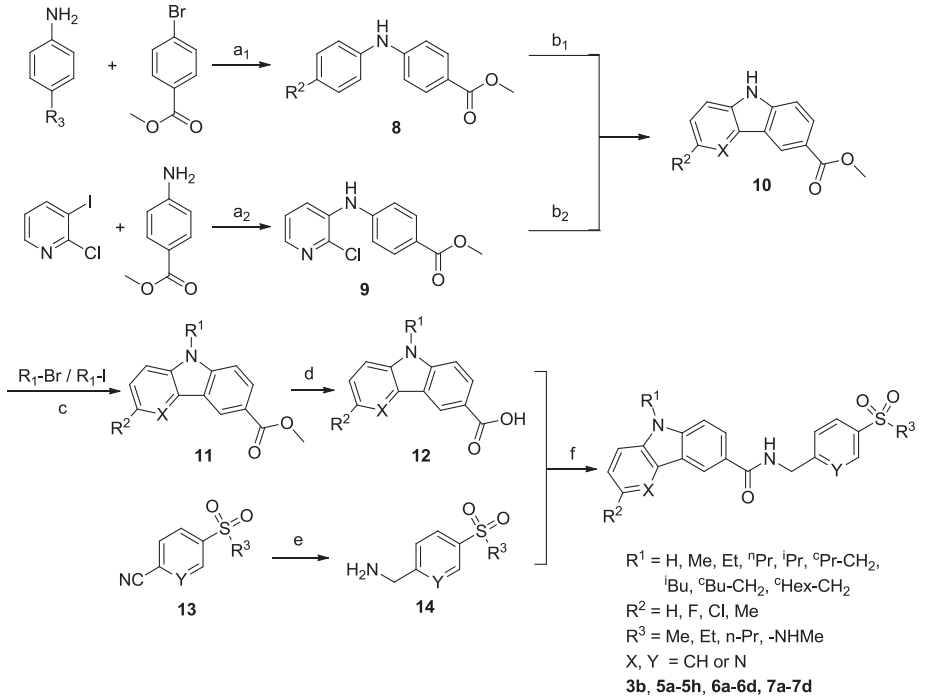


**Scheme 1.** General synthetic procedures for carbazolyl carboxamides analogues.

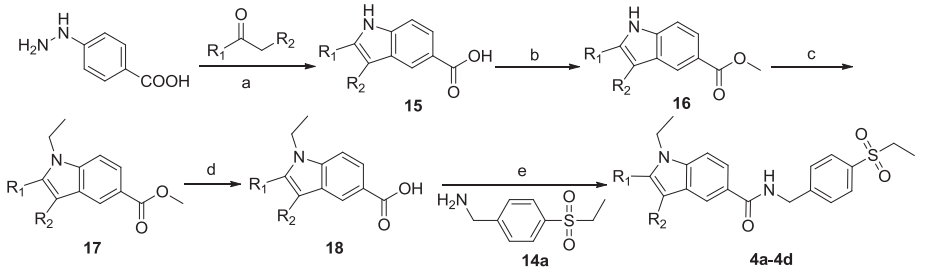


**Scheme 2.** General synthetic procedures for non-carbazolyl carboxamides analogues.

were reduced. In view of the RORγt activity and the potential genotoxicity of **3a** associated with its aniline moiety, we selected the reversed amide linker in **3b** as the preferred linker for further LHS and RHS optimization.

We subsequently explored the LHS SAR of the carbazole carboxamide **3b**. Results were summarized in Table 2. Changing carbazole ring (**3b**) to tetrahydrocarbazole ring (**4a**) lowered RORγt activity. Reducing the size of the tetrahydrocarbazole ring to indole ring and its derivatives (**4b-4d**) further lowered the RORγt activity although the MW and cLogPs of these indole derivatives were reduced, indicating the importance of occupying a hydrophobic pocket by the larger carbazole moiety of **3b**. Not surprisingly, the size of substituents on nitrogen of the carbazole ring modulated the RORγt activity (**3b**, **5a-5h**). The RORγt inhibitory potency ($IC_{50}$) and ligand lipophilicity (cLogP) were generally increased with the size of substituents, with an order of H ≪ Me < *i*-Pr < Et < Pr < *c*-$PrCH_2$ < *i*-Bu < *c*-$BuCH_2$ < *c*-$HexCH_2$. However, the percentage of RORγt maximum inhibition (% max. inh.) started to decrease when the size of *N*-substituents was larger than propyl, e.g., Pr > *c*-$PrCH_2$ > *i*-Bu > *c*-$BuCH_2$ > *c*-$HexCH_2$. This observation could be explained by the binding mode of the carbazole carboxamides in RORγt LBD (see Section 2.4). Since larger *N*-substituents lowered maximum percentage of RORγt inhibition and increased MW and cLogP, we turned our next attention to the modification of carbazole ring with an ethyl group capped on the nitrogen. Replacing the left phenyl ring of the carbazole with a pyridine ring (**6a**) dropped the RORγt activity dramatically, indicating that polar moiety in LHS of the carbazole carboxamides disfavored the RORγt activity. Introduction of a small substituent on the 6-position of the carbazole ring such as fluorine (**6b**), chlorine (**6c**) or methyl (**6d**) improved RORγt potency. For example, compound **6c** exhibited a decent RORγt potency with an $IC_{50}$ of 58.5 nM and a maximum inhibition of 161% and had reasonable MW (455) and cLogP (5.03) comparing to GSK805 (**1**) or Takeda's compound (**2**). The effect of small substituents such as Cl and Me on RORγt activity could be explained by the binding mode of the carbazole carboxamides in RORγt LBD (see section 2.4). Either Cl (**6c**) or Me (**6d**) on 6-position of the carbazole moiety was found to fit well into the hydrophobic pocket of the RORγt LBD and therefore exhibited better potency than **3b**.

Fixing the LHS moiety as *N*-ethyl carbazole, SAR of the RHS was briefly explored based on the SAR knowledge learnt from the other chemical series with the same RHS moiety [23,25], and summarized in Table 3. Changing the ethyl sulfone in **3b** with either a

**Table 1**
SAR exploration of the linkers.

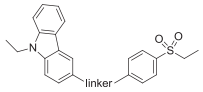


| Compd | linker | MW | cLogP | RORγ FRET $IC_{50}$ (nM)[a] (% max. inh.)[b] |
|---|---|---|---|---|
| **3a** |  | 421 | 4.16 | 170 (156) |
| **3b** |  | 421 | 4.30 | 167 (153) |
| **3c** |  | 436 | 4.37 | 16200 (61) |
| **3d** | 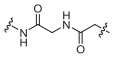 | 478 | 3.38 | 7670 (61) |
| **3e** | 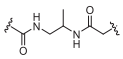 | 506 | 3.76 | N/A[c] |
| **1** | GSK805 | 532 | 5.23 | 34.0 (127) |
| **2** | Example 14 in Takeda's patent | 472 | 6.44 | 54.0 (176) |

[a] $IC_{50}$ value is the average of at least two independent determinations.
[b] Percent of maximum inhibition measured against activation by the surrogate agonist.
[c] N/A represents no activity.

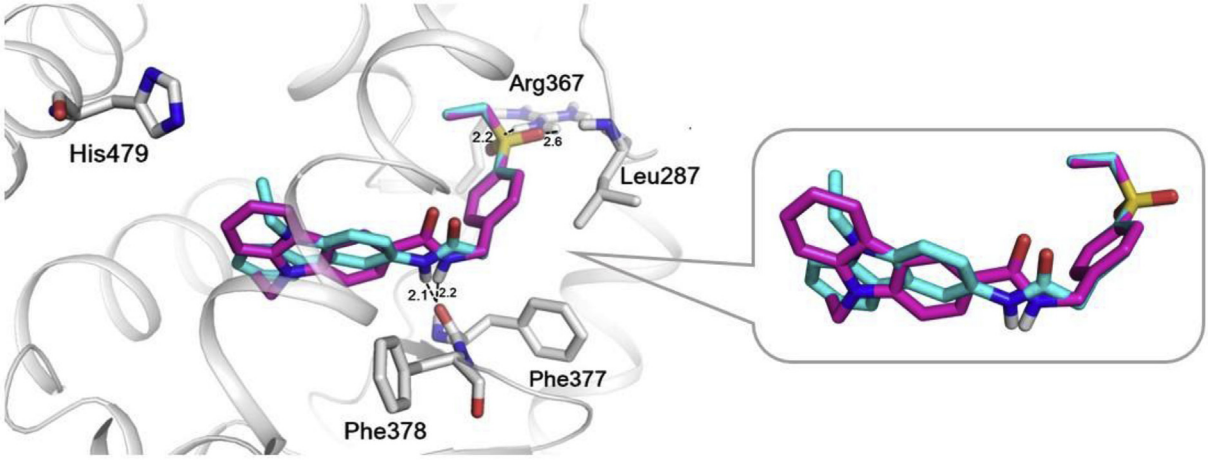


**Fig. 5.** Structural superimposition of the docked poses of **3a** (cyan stick) with **3b** (magenta stick) in RORγt LBD (PDB: 4NIE). (For interpretation of the references to colour in this figure legend, the reader is referred to the Web version of this article.)

methyl sulfone (**7a**) or a propyl sulfone (**7b**) resulted in a drop of RORγt potency no matter cLogP is lowered or increased, indicating that the ethyl group in ethylsulfone could adopt an optimal conformation to facilitate H-bonding interactions between the sulfone oxygen and Arg367. Switching ethyl sulfone to a secondary sulfonamide (**7c**) led to a lower RORγt activity. When phenylsulfone moiety was replaced by pyridylsulfone (**7d**) with reduced cLogP, the RORγt activity was greatly reduced.

We further evaluated the representative carbazole carboxamides (**3b**, **6b-6d**) in the mouse Th17 cell differentiation assay and metabolic stability assay (Table 4). All the four compounds tested showed good inhibitory activity in the Th17 cell differentiation assay and exhibited reasonable metabolic stability in mouse liver microsomes, among which **6c** stands out with an inhibition of 58.8% at 0.3 μM and intrinsic clearance of 0.197 mL/min/g (liver), respectively.

### 2.4. Binding mode study

Docking of *N*-ethyl-carbazole carboxamide (**3b**) into RORγt LBD revealed the binding mode of a typical carbazole carboxamide-based RORγt inverse agonist (Fig. 6). In the binding mode, carbazole moiety in the LHS of the amide, functioning as the biaryl moiety in **1**, provided preferred intermolecular interactions with surrounding hydrophobic residues in the hydrophobic site near Tyr502 and His479, which was believed to be important for the RORγt binding affinity. In the RHS, the sulfone moiety formed two hydrogen bonds: one with Arg367 and the other with the backbone of Leu287. The linker amide formed hydrogen bond interaction with the backbone of Phe377. In addition, two π-π stacking interactions were observed: one between the sulfone-substituted phenyl ring and Phe377, and the other between the carbazole moiety and Phe378.

**Table 2**
SAR exploration on the LHS of the carboxamides.

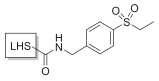


| Compd | LHS | MW | cLogP | RORγ FRET $IC_{50}$ (nM)[a] (% max. inh.)[b] |
|---|---|---|---|---|
| **3b** |  | 421 | 4.30 | 167 (153) |
| **4a** |  | 425 | 4.48 | 426 (151) |
| **4b** |  | 399 | 3.86 | 914 (152) |
| **4c** | 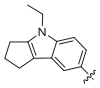 | 411 | 3.93 | 1320 (141) |
| **4d** |  | 370 | 2.91 | 5160 (134) |
| **5a** | 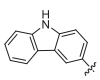 | 392 | 3.28 | 5400 (93) |
| **5b** | 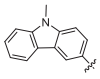 | 407 | 3.77 | 566 (140) |
| **5c** | 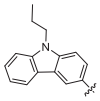 | 435 | 4.83 | 138 (150) |
| **5d** | 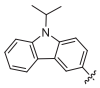 | 435 | 4.61 | 358 (126) |
| **5e** | 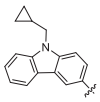 | 447 | 4.74 | 81.9 (115) |
| **5f** | 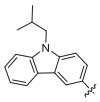 | 449 | 5.22 | 69.6 (91) |
| **5g** | 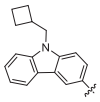 | 461 | 5.30 | 54.9 (82) |
| **5h** | 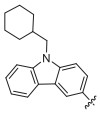 | 489 | 6.42 | 33.5 (32) |
| **6a** | 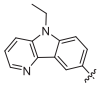 | 422 | 2.98 | 3000 (103) |
| **6b** | 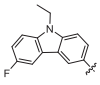 | 439 | 4.46 | 156 (149) |
| **6c** | 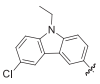 | 455 | 5.03 | 58.5 (161) |
| **6d** | 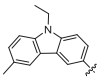 | 435 | 4.80 | 47.8 (112) |
| **1** | GSK805 | 532 | 5.23 | 34.0 (127) |
| **2** | Example 14 in Takeda's patent | 472 | 6.44 | 54.0 (176) |

[a] $IC_{50}$ value is the average of at least two independent determinations.
[b] Percent of maximum inhibition measured against activation by the surrogate agonist.

**Table 3**
SAR exploration on the RHS of the carboxamides.

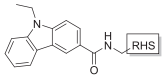


| Compd | RHS | MW | cLogP | RORγ FRET $IC_{50}$ (nM)[a] (% max. inh.)[b] |
|---|---|---|---|---|
| **3b** |  | 421 | 4.30 | 167 (153) |
| **7a** |  | 407 | 3.76 | 1100 (167) |
| **7b** |  | 435 | 4.83 | 1450 (169) |
| **7c** |  | 422 | 4.18 | 313 (161) |
| **7d** |  | 422 | 3.41 | 1220 (158) |
| **1** | GSK805 | 532 | 5.23 | 34.0 (127) |
| **2** | Example 14 in Takeda's patent | 472 | 6.44 | 54.0 (176) |

[a] $IC_{50}$ value is the average of at least two independent determinations.
[b] Percent of maximum inhibition measured against activation by the surrogate agonist.

**Table 4**
Results in Th17 cell differentiation assay and metabolic stability assay.

| Compd | mTh17, % inh.@0.3 μM | $CL_{int}$, mL/min/g (liver) |
|---|---|---|
| **3b** | 40.0 | 0.305 |
| **6b** | 45.9 | 0.348 |
| **6c** | 58.8 | 0.197 |
| **6d** | 43.6 | 0.368 |

In the SAR exploration, we found that when the *N*-substituent at carbazole ring is larger, the maximum percentage of inhibition of a carbazole carboxamide is lower. For example, *N*-cyclohexylmethyl carbazole carboxamide (**5h**) only had a max. inh. of 32% in RORγ FRET assay, compared to that of 153% for the *N*-ethyl counterpart (**3b**). Fig. 7a showed the predicted binding modes of **5h** compared with **3b**. The cyclohexylmethyl substituent of **5h** was found to make the carbazole ring naturally rotated 180° compared to **3b**, more extended toward helix 12 (H12) and closer to the side chain of

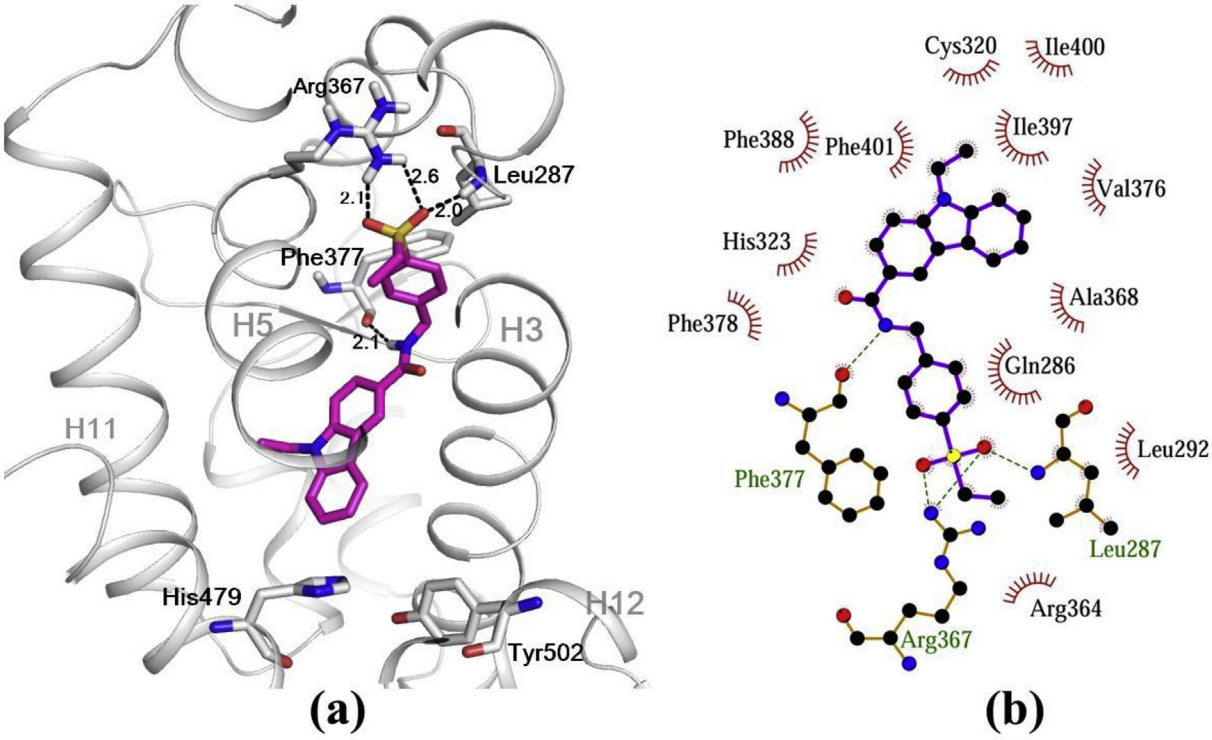


**Fig. 6.** (a) Zoomed-in view of **3b** in the binding pocket of RORγt LBD (PDB: 4NIE); (b) A two-dimensional plot showing the interactions between **3b** and the surrounding amino acids.

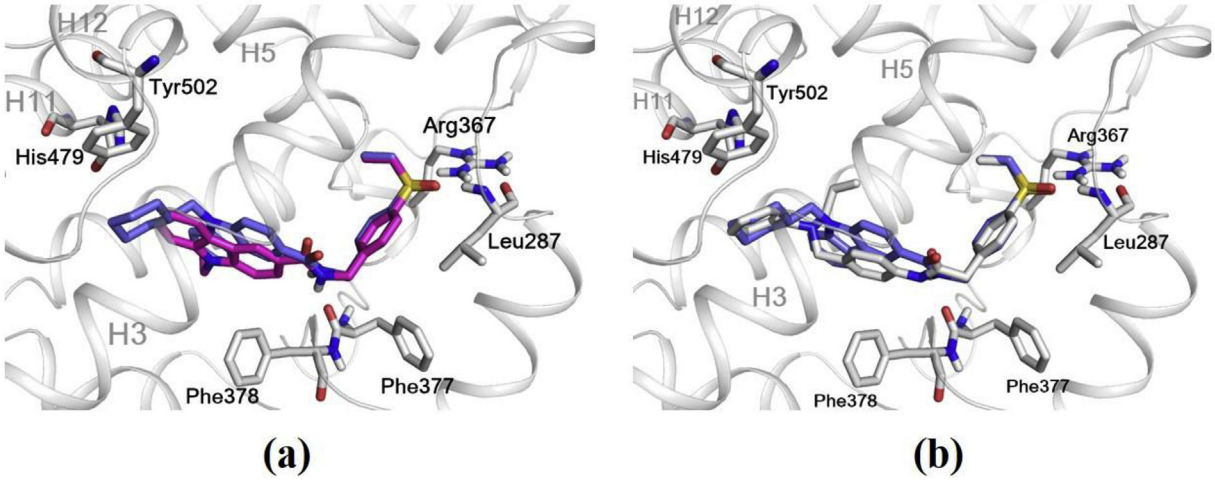


**Fig. 7.** (a) Structural superimposition of **3b** (magenta stick) and **5h** (slate stick); (b) Structural superimposition of **5h** (slate) and the RORγt agonist (grey) in co-crystal structure of 4NIE. (For interpretation of the references to colour in this figure legend, the reader is referred to the Web version of this article.)

His479 and Tyr502 on H12 in a low energy conformation. Overlay of **5h** with the previously discovered agonist (*N*-(4-((benzyl(propyl) amino)methyl)phenyl)-2-(4-(ethylsulfonyl)phenyl)acetamide [24]) in RORγt co-crystal structure (PDB: 4NIE) (Fig. 7b) indicated that the *N*-cyclohexylmethyl moiety occupied almost the same place of the agonist's benzyl group, being able to partially stabilize the activation function 2 (AF2) domain (H12) toward recruitment of steroid receptor co-activator (SRC) and possibly make **5h** a partial agonist. To confirm, we tested **5h** in a dual FRET assay (without adding a surrogate agonist) and found it indeed a partial agonist with a $EC_{50}$ of 18 nM and maximum activation of 54%. Binding modes of the carbazole carboxamides in RORγt LBD accord with our understanding of agonist/inverse agonist conversion in the aryl amide-based RORγt modulators [23,24,30].

## 3. Conclusions

In summary, we have discovered a series of carbazole carboxamides as novel RORγt inverse agonists by a scaffold hybridization strategy. Structure-activity relationship exploration on the amide linker, the LHS carbazole ring and the RHS arylsulfone moiety of the hybrid amide **3a** led to the identification of potent RORγt inverse

agonists. Compound **6c** was found to have good RORγt activity in both FRET assay and mouse Th17 cell differentiation assays as well as reasonable metabolic stability in mouse liver microsomes. Further optimization of the carbazole carboxamide lead series with the aid of the binding mode study is undergoing.

## 4. Experimental

### 4.1. Materials and methods

All the reagents used were commercially available and were used without further purification unless otherwise indicated. Microwave reaction was conducted with a Biotage Initiator™ microwave synthesizer. Melting point was recorded by WRS-1B digital instrument. Analytical thin-layer chromatography and preparative thin-layer chromatography were performed with silica gel plates using silica gel 60 GF254 (Qingdao Haiyang Chemical Co., Ltd., Qingdao, Shandong Province, China). $^1$H NMR spectra were recorded in DMSO-d6, $CD_3OD$ or $CDCl_3$ solution on a Bruker 400 MHz spectrometer, with chemical shifts expressed in parts per million using tetramethylsilane (TMS) as an internal standard. Mass spectroscopy was carried out on Electrospray ionization (ESI) instruments or MALDI-TOF (Bruker).

### 4.2. Synthesis

#### 4.2.1. General procedure A for the synthesis of carbazole carboxamides analogues (**3b**, **5a**-**5h**, **6b**-**6d**, **7a**-**7d**)

**Step 1:** To a sealed vial was added aniline (1.2 eq), methyl 4-(phenylamino)benzoate (1 eq), $Pd(OAc)_2$ (0.05 mmol), rac-BINAP (0.05 eq), $K_2CO_3$ (3 eq) and toluene. Then the sealed vial was irradiated in the microwave at 130 °C for 2 h. After the reaction completed, ethyl acetate was added to dilute the reaction mixture, and then filtered by diatomite. The filtrate was concentrated under reduced pressure and the residue was purified by column chromatography on silica gel to afford diphenylamine intermediate (**8**).

**Step 2:** To a solution of diphenylamine (1 eq) in acetic acid was added $Pd(OAc)_2$ (1.1 eq). The mixture was stirred under $N_2$ at 120 °C for 1 h. After the reaction was complete, acetic acid was removed under reduced pressure. The residue was purified by column chromatography on silica gel to afford methyl 9*H*-carbazole-3-carboxylate intermediate (**10**).

**Step 3:** To a stirred solution of methyl 9*H*-carbazole-3-carboxylate (1 eq) in DMF was added NaH (3 eq) at 0 °C. The reaction mixture was stirred at 0 °C for 30 min, and then bromides or iodides (3 eq) were added. The mixture was reacted at room temperature until the reaction completed. Water was added to quench the reaction and the mixture was extracted with ethyl acetate several times. Then the organic layer was combined and the solvent was removed under reduced pressure to afford substituted carbazole carboxylate intermediate (**11**).

**Step 4:** To a stirred solution of substituted carbazole carboxylate (1 eq) in ethanol/$H_2O$ (5:1) was added LiOH or KOH (3 eq). The mixture was stirred at 90 °C. After the reaction completed, ethanol was removed under reduced pressure. Then pH of the mixture was adjusted to 3 with 2 *N* hydrochloric acid solution. The mixture was filtered to afford the carbazole carboxylic acid intermediate (**12**) as solid.

**Step 5:** To a stirred solution of carbazole carboxylic acid (1 eq) in DCM was added HATU (1.2 eq), *N*,*N*-diisopropylethylamine (3 eq) and benzylamine (1.2 eq). The mixture was stirred at room temperature. After the reaction completed, solvent was removed under reduced pressure, and the residue was purified by column chromatography on silica gel to afford the target compounds (**3b**, **5a**-**5h**, **6b**-**6d**, **7a**-**7d**).

*4.2.1.1. 9-Ethyl-N-(4-(ethylsulfonyl)benzyl)-9H-carbazole-3-carboxamide (**3b**).* Off white solid (71%); mp 161.3–162.3 °C. $^1$H NMR (400 MHz, $CD_3OD$) δ 8.70 (s, 1H), 8.15 (d, *J* = 7.7 Hz, 1H), 8.03 (d, *J* = 8.7 Hz, 1H), 7.89 (d, *J* = 8.3 Hz, 2H), 7.66 (d, *J* = 8.2 Hz, 2H), 7.61–7.54 (m, 2H), 7.50 (t, *J* = 7.6 Hz, 1H), 7.26 (t, *J* = 7.3 Hz, 1H), 4.75 (s, 2H), 4.47 (q, *J* = 7.1 Hz, 2H), 3.19 (q, *J* = 7.4 Hz, 2H), 1.42 (t, *J* = 7.2 Hz, 3H), 1.20 (t, *J* = 7.4 Hz, 3H). $^{13}$C NMR (151 MHz, DMSO-d6) δ 167.41, 146.88, 141.73, 140.67, 137.34, 128.45, 128.41, 126.74, 125.70, 125.15, 122.81, 122.23, 120.87, 120.55, 119.94, 110.02, 109.12, 49.74, 42.94, 37.66, 14.16, 7.64. MS (ESI) *m*/*z*: 421.1 $[M+H]^+$. HRMS ($ESI^+$) *m*/*z* calcd for $C_{24}H_{24}N_2O_3S$ $[M+H]^+$: 421.1580; found: 421.1575.

*4.2.1.2. N-(4-(Ethylsulfonyl)benzyl)-9H-carbazole-3-carboxamide (**5a**).* Off white solid (38.1%); mp 185.0–187.0 °C. $^1$H NMR (400 MHz, $CD_3OD$) δ 8.68 (d, *J* = 1.2 Hz, 1H), 8.12 (d, *J* = 7.8 Hz, 1H), 7.96 (d, *J* = 8.5, 1.7 Hz, 1H), 7.89 (d, *J* = 8.3 Hz, 2H), 7.67 (d, *J* = 8.3 Hz, 2H), 7.49 (t, *J* = 8.0 Hz, 2H), 7.42 (t, *J* = 7.7 Hz, 1H), 7.22 (t, *J* = 7.4 Hz, 1H), 4.74 (s, 2H), 3.19 (q, *J* = 7.4 Hz, 2H), 1.20 (t, *J* = 7.4 Hz, 3H). $^{13}$C NMR (151 MHz, $CD_3OD$) δ 169.76, 146.13, 142.26, 140.77, 137.06, 128.11, 127.85, 125.97, 124.68, 124.01, 122.89, 122.76, 119.76, 119.49, 119.17, 110.75, 110.10, 49.87, 42.77, 6.18. MS (ESI) *m*/*z*: 393.0$[M+H]^+$. HRMS ($ESI^+$) *m*/*z* calcd for $C_{22}H_{20}N_2O_3S$ $[M+H]^+$: 393.1267; found: 393.1259.

*4.2.1.3. N-(4-(Ethylsulfonyl)benzyl)-9-methyl-9H-carbazole-3-carboxamide (**5b**).* Off white solid(10.2%); mp 178.6–180.3 °C. $^1$H NMR (400 MHz, $CD_3OD$) δ 8.70 (s, 1H), 8.15 (d, *J* = 7.7 Hz, 1H), 8.04 (dd, *J* = 8.6, 1.7 Hz, 1H), 7.89 (d, *J* = 8.4 Hz, 2H), 7.67 (d, *J* = 8.4 Hz, 2H), 7.57 (m, 2H), 7.51 (t, *J* = 7.9 Hz, 1H), 7.27 (t, *J* = 6.7 Hz, 1H), 4.75 (s, 2H), 3.92 (s, 3H), 3.20 (q, *J* = 7.4 Hz, 2H), 1.21 (t, *J* = 7.4 Hz, 3H). $^{13}$C NMR (151 MHz, DMSO-d6) δ 166.77 (s), 146.23 (s), 142.12 (s), 141.11 (s), 136.67 (s), 127.80 (d, *J* = 7.2 Hz), 126.10 (s), 125.06 (s), 124.47 (s), 121.96 (s), 121.37 (s), 120.09 (s), 119.80 (s), 119.34 (s), 109.44 (s), 108.54 (s), 49.08 (s), 42.30 (s), 29.04 (s), 7.01 (s). MS (ESI) *m*/*z*: 407.0 $[M+H]^+$. HRMS ($ESI^+$) *m*/*z* calcd for $C_{23}H_{22}N_2O_3S$ $[M+H]^+$: 407.1424; found: 407.1412.

*4.2.1.4. N-(4-(Ethylsulfonyl)benzyl)-9-propyl-9H-carbazole-3-carboxamide (**5c**).* Off white solid (12.7%); mp 149.0–151.0 °C. $^1$H NMR (400 MHz, $CD_3OD$) δ 8.70 (d, *J* = 1.4 Hz, 1H), 8.15 (d, *J* = 7.6 Hz, 1H), 8.03 (dd, *J* = 8.7, 1.8 Hz, 1H), 7.89 (d, *J* = 8.4 Hz, 2H), 7.67 (d, *J* = 8.5 Hz, 2H), 7.60–7.55 (m, 2H), 7.50 (t, *J* = 8.0 Hz, 1H), 7.26 (t, *J* = 8.0 Hz, 1H), 4.75 (s, 2H), 4.39 (t, *J* = 7.1 Hz, 2H), 3.19 (q, *J* = 7.4 Hz, 2H), 1.96–1.87 (m, 2H), 1.20 (t, *J* = 7.1 Hz, 3H), 0.95 (t, *J* = 8 Hz, 3H). $^{13}$C NMR (151 MHz, $CD_3OD$) δ 169.60, 146.09, 142.54, 141.21, 137.07, 128.11, 127.87, 126.09, 124.81, 124.08, 122.68, 122.46, 119.92, 119.55, 119.34, 109.11, 108.44, 49.87, 44.05, 42.79, 21.90, 10.43, 6.18. MS (ESI) *m*/*z*: 435.0$[M+H]^+$. HRMS ($ESI^+$) *m*/*z* calcd for $C_{25}H_{26}N_2O_3S$ $[M+H]^+$: 435.1737; found: 435.1730.

*4.2.1.5. N-(4-(Ethylsulfonyl)benzyl)-9-isopropyl-9H-carbazole-3-carboxamide (**5d**).* Off white solid (35.4%); mp 138.8–140.8 °C.$^1$H NMR (400 MHz, $CD_3OD$) δ 8.70 (d, *J* = 1.6 Hz, 1H), 8.15 (d, *J* = 7.8 Hz, 1H), 8.00 (dd, *J* = 8.7, 1.8 Hz, 1H), 7.89 (d, *J* = 8.3 Hz, 2H), 7.70–7.65 (m, 4H), 7.47 (t, *J* = 7.3 Hz, 1H), 7.24 (t, *J* = 7.5 Hz, 1H), 5.18–5.08 (m, 1H), 4.74 (s, 2H), 3.19 (q, *J* = 7.4 Hz, 2H), 1.71 (d, *J* = 7.0 Hz, 6H), 1.20 (t, *J* = 7.4 Hz, 3H). $^{13}$C NMR (151 MHz, $CD_3OD$) δ 169.50, 146.06, 141.45, 140.15, 137.04, 128.09, 127.88, 125.90, 124.59, 123.84, 123.18, 122.97, 119.95, 119.51, 119.20, 110.37, 109.59, 49.85, 46.89, 42.78, 19.52, 6.18. MS (ESI) *m*/*z*: 435.0 $[M+H]^+$. HRMS ($ESI^+$) *m*/*z* calcd for $C_{25}H_{26}N_2O_3S$ $[M+H]^+$: 435.1737; found: 435.1731.

*4.2.1.6. 9-(Cyclopropylmethyl)-N-(4-(ethylsulfonyl)benzyl)-9H-carbazole-3-carboxamide (**5e**).* Off white solid (38.3%); mp

177.6–179.6 °C.$^1$H NMR (400 MHz, $CD_3OD$) δ 8.70 (d, $J$ = 1.3 Hz, 1H), 8.14 (d, $J$ = 7.7 Hz, 1H), 8.02 (d, $J$ = 8.6, 1.7 Hz, 1H), 7.88 (d, $J$ = 8.3 Hz, 2H), 7.66 (d, $J$ = 8.3 Hz, 2H), 7.61–7.57 (m, 2H), 7.49 (t, $J$ = 7.7 Hz, 1H), 7.25 (t, $J$ = 7.5 Hz, 1H), 4.74 (s, 2H), 4.33 (d, $J$ = 6.6 Hz, 2H), 3.18 (q, $J$ = 7.4 Hz, 2H), 1.38–1.32 (m, 1H), 1.20 (t, $J$ = 7.4 Hz, 3H), 0.56–0.48 (m, 2H), 0.48–0.41 (m, 2H). $^{13}$C NMR (151 MHz, DMSO-d6) δ 167.40, 146.88, 142.32, 141.25, 137.33, 128.44, 128.40, 126.73, 125.67, 125.14, 122.73, 122.15, 120.76, 120.46, 119.94, 110.43, 109.53, 49.73, 46.77, 42.93, 11.20, 7.64, 4.06. MS (ESI) $m/z$: 447.0 $[M+H]^+$. HRMS ($ESI^+$) $m/z$ calcd for $C_{26}H_{26}N_2O_3S$ $[M+H]^+$:447.1737; found: 447.1752.

*4.2.1.7. N-(4-(Ethylsulfonyl)benzyl)-9-isobutyl-9H-carbazole-3-carboxamide (**5f**).* Off white solid (20.2%); mp 166.4–168.4 °C. $^1$H NMR (400 MHz, $CD_3OD$) δ 8.71 (d, $J$ = 1.4 Hz, 1H), 8.16 (d, $J$ = 7.8 Hz, 1H), 8.02 (dd, $J$ = 8.7, 1.8 Hz, 1H), 7.90 (d, $J$ = 8.4 Hz, 2H), 7.67 (d, $J$ = 8.4 Hz, 2H), 7.59–7.54 (m, 2H), 7.49 (t, $J$ = 7.6 Hz, 1H), 7.26 (t, $J$ = 7.4 Hz, 1H), 4.75 (s, 2H), 4.22 (d, $J$ = 7.5 Hz, 2H), 3.20 (q, $J$ = 7.4 Hz, 2H), 2.46–2.31 (m, 1H), 1.21 (t, $J$ = 7.4 Hz, 3H), 0.97 (d, $J$ = 6.7 Hz, 6H). $^{13}$C NMR (151 MHz, DMSO-d6) δ 167.41, 146.88, 142.61, 141.50, 137.33, 128.43, 128.40, 126.66, 125.61, 125.11, 122.61, 122.00, 120.74, 120.43, 119.91, 110.57, 109.69, 50.14, 49.74, 42.93, 28.84, 20.50, 7.64. MS (ESI) $m/z$: 448.9$[M+H]^+$. HRMS ($ESI^+$) $m/z$ calcd for $C_{26}H_{28}N_2O_3S$ $[M+H]^+$: 449.1893; found: 449.1906.

*4.2.1.8. 9-(Cyclobutylmethyl)-N-(4-(ethylsulfonyl)benzyl)-9H-carbazole-3-carboxamide (**5g**).* Off white solid (58.3%). mp 203.5–205.5 °C .$^1$H NMR (400 MHz, $CD_3OD$) δ 8.70 (s, 1H), 8.14 (d, $J$ = 7.8 Hz, 1H), 8.02 (d, $J$ = 8.6 Hz, 1H), 7.89 (d, $J$ = 8.2 Hz, 2H), 7.67 (d, $J$ = 8.2 Hz, 2H), 7.63–7.57 (m, 2H), 7.49 (t, $J$ = 7.6 Hz, 1H), 7.25 (t, $J$ = 7.4 Hz, 1H), 4.75 (d, $J$ = 4.5 Hz, 2H), 4.43 (s, 2H), 3.19 (q, $J$ = 7.4 Hz, 2H), 2.98–2.95 (m, 1H), 2.01–1.96 (m, 2H), 1.93–1.89 (m, 4H), 1.21 (t, $J$ = 7.4 Hz, 3H). $^{13}$C NMR (151 MHz, DMSO-d6) δ 167.40, 146.88, 142.52, 141.43, 137.33, 128.44, 128.40, 126.67, 125.63, 125.11, 122.62, 122.03, 120.73, 120.43, 119.91, 110.38, 109.49, 49.74, 47.56, 42.93, 38.72, 35.62, 26.31, 18.40, 7.64. MS (ESI) $m/z$: 461.0 $[M+H]^+$. HRMS ($ESI^+$) $m/z$ calcd for $C_{27}H_{28}N_2O_3S$ $[M+H]^+$: 461.1893; found: 461.1908.

*4.2.1.9. 9-(Cyclohexylmethyl)-N-(4-(ethylsulfonyl)benzyl)-9H-carbazole-3-carboxamide (**5h**).* Off white solid (8.0%); mp 190.2–192.0 °C. $^1$H NMR (400 MHz, $CDCl_3$) δ 8.61 (s, 1H), 8.12 (d, $J$ = 7.7 Hz, 1H), 7.94 (d, $J$ = 8.6 Hz, 1H), 7.87 (d, $J$ = 8.1 Hz, 2H), 7.59 (d, $J$ = 8.2 Hz, 2H), 7.51 (t, $J$ = 7.5 Hz, 1H), 7.43 (d, $J$ = 10.7 Hz, 2H), 7.29 (d, $J$ = 7.6 Hz, 1H), 6.76 (t, $J$ = 5.3 Hz, 1H), 4.82 (d, $J$ = 5.7 Hz, 2H), 4.14 (d, $J$ = 7.3 Hz, 2H), 3.10 (q, $J$ = 7.4 Hz, 2H), 2.00 (m, 1H), 1.66 (m, 10H), 1.28 (t, $J$ = 7.4 Hz, 3H). $^{13}$C NMR (151 MHz, $CD_3OD$) δ 169.51, 147.04, 143.54, 142.31, 138.00, 128.97, 128.74, 127.03, 125.85, 125.20, 123.39, 122.91, 120.89, 120.50, 120.27, 110.60, 109.86, 50.56, 49.68, 43.49, 31.59, 26.79, 26.32, 7.32. MS (ESI) $m/z$: 489.3$[M+H]^+$. HRMS ($ESI^+$) $m/z$ calcd for $C_{29}H_{32}N_2O_3S$ $[M+H]^+$: 489.2206; found: 489.2217.

*4.2.1.10. 9-Ethyl-N-(4-(ethylsulfonyl)benzyl)-6-fluoro-9H-carbazole-3-carboxamide (**6b**).* Off white solid (69.4%); mp 166.8–170.9 °C. $^1$H NMR (400 MHz, $CDCl_3$) δ 8.56 (s, 1H), 7.97 (d, $J$ = 8.7 Hz, 1H), 7.87 (d, $J$ = 8.2 Hz, 2H), 7.77 (dd, $J$ = 8.6, 2.4 Hz, 1H), 7.58 (d, $J$ = 8.2 Hz, 2H), 7.43 (d, $J$ = 8.5 Hz, 1H), 7.36 (dd, $J$ = 8.8, 4.1 Hz, 1H), 7.25–7.22 (m, 1H), 6.79 (s, 1H), 4.82 (d, $J$ = 5.7 Hz, 2H), 4.37 (t, $J$ = 7.2 Hz, 2H), 3.10 (q, $J$ = 7.4 Hz, 2H), 1.44 (t, $J$ = 7.2 Hz, 3H), 1.28 (d, $J$ = 7.4 Hz, 3H).$^{13}$C NMR (151 MHz, DMSO-d6) δ 166.71, 157.49, 155.94, 146.18, 141.90), 136.68, 136.51, 127.80), 127.78,125.46, 124.55, 122.72, 122.66, 121.21, 120.68, 113.80, 113.64, 110.51, 110.45, 108.80, 106.11, 105.96, 49.08, 42.29, 37.23, 13.54), 7.01. MS (ESI) $m/z$: 435.2 $[M+H]^+$. HRMS ($ESI^+$) $m/z$ calcd for $C_{24}H_{23}FN_2O_3S$ $[M+H]^+$: 439.1486; found: 439.1500.

*4.2.1.11. 6-Chloro-9-ethyl-N-(4-(ethylsulfonyl)benzyl)-9H-carbazole-3-carboxamide (**6c**).* Off white solid (77.8%); mp 155.8–157.9 °C. $^1$H NMR (400 MHz, DMSO-d6) δ 9.11 (t, $J$ = 5.9 Hz, 1H), 8.80 (s, 1H), 8.26 (d, $J$ = 1.9 Hz, 1H), 8.09–8.02 (m, 1H), 7.84 (d, $J$ = 8.3 Hz, 2H), 7.71 (d, $J$ = 3.3 Hz, 2H), 7.69 (d, $J$ = 3.3 Hz, 2H), 7.61 (d, $J$ = 8.3 Hz, 2H), 7.50 (dd, $J$ = 8.7, 2.0 Hz, 1H), 4.63 (d, $J$ = 5.8 Hz, 2H), 4.47 (q, $J$ = 6.9 Hz, 2H), 3.24 (q, $J$ = 7.4 Hz, 2H), 1.29 (t, $J$ = 7.1 Hz, 3H), 1.07 (t, $J$ = 7.4 Hz, 3H). $^{13}$C NMR (151 MHz, DMSO-d6) δ 167.30, 146.78, 142.21, 139.14, 137.36, 128.46, 128.41, 126.49, 126.32, 125.66, 124.34, 124.12, 121.36, 121.25, 120.53, 111.64, 109.51, 49.73, 42.94, 37.89, 14.15, 7.64. MS (ESI) $m/z$: 454.9$[M+H]^+$. HRMS ($ESI^+$) $m/z$ calcd for $C_{24}H_{23}ClN_2O_3S$ $[M+H]^+$: 455.1191; found: 455.1207.

*4.2.1.12. 9-Ethyl-N-(4-(ethylsulfonyl)benzyl)-6-methyl-9H-carbazole-3-carboxamide (**6d**).* Off white solid (69.4%); mp 160.4–161.5 °C.$^1$H NMR (400 MHz, $CDCl_3$) δ 8.62 (s, 1H), 7.96 (dd, $J$ = 8.6, 1.3 Hz, 1H), 7.87 (s, 1H), 7.74 (d, $J$ = 8.2 Hz, 2H), 7.48 (d, $J$ = 8.2 Hz, 2H), 7.35 (d, $J$ = 8.6 Hz, 1H), 7.32–7.27 (m, 3H), 4.74 (d, $J$ = 5.9 Hz, 2H), 4.32 (q, $J$ = 7.2 Hz, 2H), 3.05 (q, $J$ = 7.4 Hz, 2H), 2.49 (s, 3H), 1.39 (t, $J$ = 7.2 Hz, 3H), 1.24 (d, $J$ = 7.4 Hz, 3H). $^{13}$C NMR (151 MHz, DMSO-d6) δ 167.41, 146.89, 141.91, 139.00, 137.34, 128.75, 128.44, 128.40, 128.01, 125.53, 124.86, 122.95, 122.03, 120.68, 120.44, 109.77, 109.02, 49.74, 42.92, 37.66, 21.51, 14.16, 7.64. MS (ESI) $m/z$: 435.2$[M+H]^+$. HRMS ($ESI^+$) $m/z$ calcd for $C_{25}H_{26}N_2O_3S$ $[M+H]^+$: 435.1737; found: 435.1744.

*4.2.1.13. 9-Ethyl-N-(4-(methylsulfonyl)benzyl)-9H-carbazole-3-carboxamide (**7a**).* Off white solid (48.5%); mp 206.4–208.1 °C.$^1$H NMR (400 MHz, DMSO-d6) δ 9.15 (t, $J$ = 5.8 Hz, 1H), 8.75 (s, 1H), 8.17 (d, $J$ = 7.7 Hz, 1H), 8.07–8.00 (m, 1H), 7.88 (d, $J$ = 8.3 Hz, 2H), 7.70–7.62 (m, 2H), 7.60 (d, $J$ = 8.3 Hz, 2H), 7.49 (t, $J$ = 7.7 Hz, 1H), 7.24 (t, $J$ = 7.4 Hz, 1H), 4.62 (d, $J$ = 5.8 Hz, 2H), 4.47 (q, $J$ = 7.0 Hz, 2H), 3.17 (s, 3H), 1.31 (t, $J$ = 7.1 Hz, 3H). $^{13}$C NMR (151 MHz, DMSO-d6) δ 167.39, 146.72, 141.72, 140.66, 139.70, 128.46, 127.55, 126.74, 125.69, 125.16, 122.80, 122.22, 120.87, 120.53, 119.94, 110.02, 109.12, 44.13, 42.96, 37.66, 14.16. MS (ESI) $m/z$: 407.0 $[M+H]^+$. HRMS ($ESI^+$) $m/z$ calcd for $C_{23}H_{22}N_2O_3S$ $[M+H]^+$: 407.1424; found: 407.1434.

*4.2.1.14. 9-Ethyl-N-(4-(propylsulfonyl)benzyl)-9H-carbazole-3-carboxamide (**7b**).* Off white solid (40.2%); mp 150.8–152.5 °C .$^1$H NMR (400 MHz, $CDCl_3$) δ 8.63 (s, 1H), 8.12 (d, $J$ = 7.8 Hz, 1H), 7.97 (d, $J$ = 8.6 Hz, 1H), 7.82 (d, $J$ = 8.1 Hz, 2H), 7.55 (d, $J$ = 8.2 Hz, 2H), 7.51 (d, $J$ = 7.9 Hz, 1H), 7.47–7.40 (m, 2H), 7.28 (d, $J$ = 7.3 Hz, 1H), 6.93 (s, 1H), 4.80 (d, $J$ = 5.6 Hz, 2H), 4.39 (q, $J$ = 7.2 Hz, 2H), 3.08–3.00 (m, 2H), 1.75–1.69 (m, 2H), 1.45 (t, $J$ = 7.2 Hz, 3H), 0.97 (t, $J$ = 7.4 Hz, 3H). $^{13}$C NMR (151 MHz, DMSO-d6) δ 167.41, 146.84, 141.73, 140.67, 137.94, 128.44, 128.28, 126.74, 125.70, 125.15, 122.81, 122.23, 120.87, 120.55, 119.94, 110.02, 109.12, 56.81, 42.94, 37.66, 16.69, 14.16, 12.98. MS (ESI) $m/z$: 432.9 $[M-H]^-$, MS (ESI) $m/z$: 435.2 $[M+H]^+$. HRMS ($ESI^+$) $m/z$ calcd for $C_{25}H_{26}N_2O_3S$ $[M+H]^+$: 435.1737; found: 435.1749.

*4.2.1.15. 9-Ethyl-N-(4-(N-methylsulfamoyl)benzyl)-9H-carbazole-3-carboxamide (**7c**).* Off white solid (31.2%); mp 226.0–228.0 °C.$^1$H NMR (400 MHz, DMSO-d6) δ 9.12 (t, $J$ = 6.0 Hz, 1H), 8.76 (s, 1H), 8.17 (d, $J$ = 7.7 Hz, 1H), 8.04 (d, $J$ = 8.6 Hz, 1H), 7.73 (d, $J$ = 8.2 Hz, 2H), 7.70–7.62 (m, 2H), 7.55 (d, $J$ = 8.1 Hz, 2H), 7.49 (t, $J$ = 7.7 Hz, 1H), 7.40 (q, $J$ = 4.8 Hz, 1H), 7.24 (t, $J$ = 7.5 Hz, 1H), 4.60 (d, $J$ = 5.8 Hz, 2H), 4.47 (q, $J$ = 6.9 Hz, 2H), 2.37 (d, $J$ = 5.0 Hz, 3H), 1.31 (t, $J$ = 7.0 Hz, 3H). $^{13}$C NMR (151 MHz, DMSO-d6) δ 167.37, 145.34, 141.71, 140.66, 138.13, 128.27, 127.26, 126.73, 125.70, 125.19, 122.81, 122.21, 120.87, 120.54, 119.93, 110.02, 109.11, 42.99, 37.56, 29.20, 14.16. MS (ESI) $m/z$: 422.1$[M+H]^+$. HRMS ($ESI^+$) $m/z$ calcd for $C_{23}H_{23}N_3O_3S$ $[M+H]^+$: 422.1533; found: 422.1549.

*4.2.1.16. 9-Ethyl-N-((5-(ethylsulfonyl)pyridin-2-yl)methyl)-9H-carbazole-3-carboxamide (**7d**).* Off white solid (17.0%); mp 167.3–169.3 °C. $^1$H NMR (400 MHz, $CD_3OD$) δ 8.99 (d, *J* = 1.7 Hz, 1H), 8.73 (d, *J* = 1.1 Hz, 1H), 8.26 (dd, *J* = 8.3, 2.2 Hz, 1H), 8.15 (d, *J* = 7.8 Hz, 1H), 8.05 (dd, *J* = 8.6, 1.6 Hz, 1H), 7.68 (d, *J* = 8.3 Hz, 1H), 7.61–7.53 (m, 2H), 7.50 (t, *J* = 7.6 Hz, 1H), 7.25 (t, *J* = 7.4 Hz, 1H), 4.85 (s, 2H), 4.46 (q, *J* = 7.1 Hz, 2H), 3.26 (q, *J* = 7.4 Hz, 2H), 1.41 (t, *J* = 7.2 Hz, 3H), 1.24 (t, *J* = 7.4 Hz, 3H).$^{13}$C NMR (151 MHz, DMSO-d6) δ 166.92 (s), 164.84 (s), 147.86 (s), 141.13 (s), 140.03 (s), 136.58 (s), 133.02 (s), 126.13 (s), 125.08 (s), 124.31 (s), 122.16 (s), 121.59 (s), 121.16 (s), 120.24 (s), 120.00 (s), 119.34 (s), 109.41 (s), 108.52 (s), 49.27 (s), 44.77(s), 37.03 (s), 13.54 (s), 6.82 (s). MS (ESI) *m*/*z*: 423.1 $[M+H]^+$. HRMS ($ESI^+$) *m*/*z* calcd for $C_{23}H_{23}N_3O_3S$ $[M+Na]^+$: 444.1352; found: 444.1363.

*4.2.2. General procedure B for the synthesis of 5-ethyl-N-(4-(ethylsulfonyl)benzyl)-5H-pyrido [3,2-b]indole-8-carboxamide (**6a**)*

**Step1:** To a sealed vial was added 2-chloro-3-iodopyridine (1 eq), ethyl 4-aminobenzoate (1.2 eq), $Pd(OAc)_2$ (0.06 eq), $Cs_2CO_3$ (3 eq), rac-BINAP (0.05 eq) and toluene. Then the sealed vial was irradiated in the microwave 140 °C for 1.5 h. After the reaction completed, ethyl acetate was added to dilute the reaction mixture, and then filtered by diatomite. The filtrate was concentrated under reduced pressure, and the residue was purified by column chromatography on silica gel to afford ethyl 4-((2-chloropyridin-3-yl) amino)benzoate (**9**). $^1$H NMR (400 MHz, $CDCl_3$) δ 8.05–7.93 (m, 3H), 7.69 (d, *J* = 7.9 Hz, 1H), 7.18 (dd, *J* = 8.0, 4.6 Hz, 1H), 7.12 (d, *J* = 8.7 Hz, 2H), 6.35 (s, 1H), 4.35 (t, *J* = 7.1 Hz, 2H), 1.38 (t, *J* = 7.1 Hz, 3H).

**Step 2:** To a sealed vial was added ethyl 4-((2-chloropyridin-3-yl)amino)-benzoate (1 eq), $NaOAc\cdot 3H_2O$ (2.5 eq), $PdCl_2(PPh_3)_2$ (0.1 eq) and DMF. Then the sealed vial was irradiated in the microwave 180 °C for 2 h. After the reaction completed, $H_2O$ was added and the mixture was extracted with ethyl acetate three times. Organic layer was combined, washed with $H_2O$ for 5 times, and dried with $Na_2SO_4$. The solvent was removed under reduced pressure and the residue was purified by column chromatography on silica gel to afford ethyl 5*H*-pyrido[3,2-b]indole-8-carboxylate (**10**, X = N). $^1$H NMR (400 MHz, $CDCl_3$) δ 9.12 (s, 1H), 8.98 (s, 1H), 8.62 (dd, *J* = 4.7, 1.1 Hz, 1H), 8.23 (dd, *J* = 8.6, 1.6 Hz, 1H), 7.78 (dd, *J* = 8.2, 1.1 Hz, 1H), 7.48 (d, *J* = 8.6 Hz, 1H), 7.37 (dd, *J* = 8.2, 4.7 Hz, 1H), 4.39 (q, *J* = 7.1 Hz, 2H), 1.43–1.36 (m, 3H).

**Step 3:** To a stirred solution of ethyl 5*H*-pyrido[3,2-b]indole-8-carboxylate (1 eq) in DMF was added NaH (3 eq) at 0 °C. The reaction mixture was stirred at 0 °C for 30 min, and then bromides or iodides (3 eq) were added. The mixture was reacted at room temperature until the reaction completed. Water was added to quench the reaction and the mixture was extracted with ethyl acetate several times. Then the organic layer was combined and the solvent was removed under reduced pressure to afford ethyl 5-ethyl-5*H*-pyrido[3,2-b]indole-8-carboxylate (**11**, X = N). MS (ESI) *m*/*z*: 241.1 $[M+H]^+$.

**Step 4:** To a stirred solution of ethyl 5-ethyl-5*H*-pyrido[3,2-b] indole-8-carboxylate (1 eq) in ethanol/$H_2O$ (5:1) was added LiOH (3 eq). The mixture was stirred at 90 °C for 2 h. After the reaction was complete, ethanol was removed under reduced pressure. Then pH of the mixture was adjusted to 3 with 2 *N* hydrochloric acid solution. The mixture was filtered to afford 5-ethyl-5*H*-pyrido[3,2-b] indole-8-carboxylic acid (**12**, X = N) as solid.

**Step 5:** To a stirred solution of 5-ethyl-5*H*-pyrido[3,2-b]indole-8-carboxylic acid (1 eq) in DCM was added HATU (1.2 eq), *N*,*N*-diisopropylethylamine (3 eq) and (4-(ethylsulfonyl)phenyl)methanamine (1.2 eq). The mixture was stirred at room temperature. After the reaction completed, solvent was removed under reduced pressure. The residue was purified by column chromatography on silica gel to afford the target compound 5-ethyl-*N*-(4-(ethylsulfonyl)benzyl)-5*H*-pyrido[3,2-b]indole-8-carboxamide (**6a**) as a white solid (22.8%); mp 164.4–166.5 °C. $^1$H NMR (400 MHz, $CDCl_3$) δ 8.79 (s, 1H), 8.54 (d, *J* = 4.6 Hz, 1H), 8.23 (dd, *J* = 8.7, 1.7 Hz, 1H), 7.85 (d, *J* = 8.3 Hz, 2H), 7.76 (d, *J* = 8.3 Hz, 1H), 7.56 (d, *J* = 8.2 Hz, 2H), 7.53 (d, *J* = 8.7 Hz, 1H), 7.43–7.40 (m, 1H), 7.15 (t, *J* = 5.5 Hz, 1H), 4.78 (d, *J* = 5.9 Hz, 2H), 4.40 (q, *J* = 7.3 Hz, 2H), 3.10 (q, *J* = 7.4 Hz, 2H), 1.46 (t, *J* = 7.2 Hz, 3H), 1.28 (d, *J* = 7.4 Hz, 3H). $^{13}$C NMR (151 MHz, $CD_3OD$) δ 169.10, 146.01, 142.49, 141.12, 140.68, 137.11, 134.54, 128.72, 128.13, 127.91, 127.32, 125.61, 120.68, 119.83, 117.38, 109.20, 49.87, 42.82, 37.39, 12.72, 6.20. MS (ESI) *m*/*z*: 422.2 $[M+H]^+$. HRMS ($ESI^+$) *m*/*z* calcd for $C_{23}H_{23}N_3O_3S$ $[M+H]^+$: 422.1533; found: 422.1550.

*4.2.3. General procedure C for the synthesis of non-carbazolyl carboxamides analogues (**4a**-**4d**)*

**Step 1:** To a stirred solution of 4-hydrazinobenzoic acid (1 eq) in 1,4-dioxane was added ketone (1.1 eq) and concentrated hydrochloric acid. The reaction mixture was stirred at 120 °C overnight. A large amount of solid appeared and was filtered to afford the solid as indole acid (**15**).

**Step 2:** To a stirred solution of indole acid (1 eq) in methanol was added sulfuric acid. The mixture was stirred at 85 °C for 2 h. After cooled to room temperature, the mixture was neutralized by adding saturated $Na_2CO_3$ and then extracted with ethyl acetate. Organic layer was combined and solvent was removed under reduced pressure. The residue was purified by column chromatography on silica gel to afford indole carboxylate (**16**).

**Step 3:** To a stirred solution of indole carboxylate (1 eq) in DMF was added NaH (3 eq) at 0 °C. The reaction mixture was stirred at 0 °C for 30 min, and then bromides or iodides (3 eq) were added. The mixture was reacted at room temperature until the reaction completed. Water was added to quench the reaction and extracted with ethyl acetate several times. And then the organic layer was combined and the solvent was removed under reduced pressure to afford substituted indole carboxylate (**17**).

**Step 4:** To a stirred solution of substituted indole carboxylate (1 eq) in ethanol/$H_2O$ (5:1) was added LiOH or KOH (3 eq). The mixture was stirred at 90 °C. After the reaction completed, ethanol was removed under reduced pressure. And then pH of the mixture was adjusted to 3 with 2 *N* hydrochloric acid solution. The mixture was filtered to afford the indole acid (**18**) as solid.

**Step 5:** To a stirred solution of indole acid (1 eq) in DCM was added HATU (1.2 eq), *N*,*N*-diisopropylethylamine (3 eq) and benzylamine (1.2 eq). The mixture was stirred at room temperature. After the reaction completed, solvent was removed under reduced pressure. The residue was purified by column chromatography on silica gel to afford the target compound (**4a**-**4d**).

*4.2.3.1. 9-Ethyl-N-(4-(ethylsulfonyl)benzyl)-2,3,4,9-tetrahydro-1H-carbazole-6-carboxamide (**4a**).* Off yellow solid (74.7%); mp 193.3–195.3 °C.$^1$H NMR (400 MHz, $CD_3OD$) δ 8.02 (s, 1H), 7.85 (d, *J* = 8.1 Hz, 2H), 7.65 (d, *J* = 8.6 Hz, 1H), 7.61 (d, *J* = 8.1 Hz, 2H), 7.35 (d, *J* = 8.6 Hz, 1H), 4.68 (s, 2H), 4.16–4.10 (q, *J* = 7.1, 2H), 3.17 (q, *J* = 7.4 Hz, 2H), 2.73 (d, *J* = 6.1 Hz, 4H), 1.95 (d, *J* = 5.5 Hz, 2H), 1.87 (d, *J* = 5.2 Hz, 2H), 1.28 (t, *J* = 7.1 Hz, 3H), 1.19 (t, *J* = 7.4 Hz, 3H). $^{13}$C NMR (151 MHz, $CDCl_3$) δ 168.95, 145.63, 137.62, 137.19, 136.78, 128.51, 128.18, 127.21, 124.05, 119.52, 117.65, 110.71, 108.39, 50.67, 43.34, 37.67, 23.11, 23.02, 22.03, 20.96, 15.43, 7.42. MS (ESI) *m*/*z*: 425.0 $[M+H]^+$. HRMS ($ESI^+$) *m*/*z* calcd for $C_{24}H_{28}N_2O_3S$ $[M+H]^+$: 425.1893; found: 425.1889.

*4.2.3.2. 1-Ethyl-N-(4-(ethylsulfonyl)benzyl)-2,3-dimethyl-1H-indole-5-carboxamide (**4b**).* Off yellow solid (39.5%); mp 155.9–157.9 °C.$^1$H NMR (400 MHz, $CD_3OD$) δ 8.05 (s, 1H), 7.85 (d, *J* = 8.3 Hz, 2H), 7.65

(d, $J = 8.5$ Hz, 1H), 7.61 (d, $J = 8.2$ Hz, 2H), 7.33 (d, $J = 8.6$ Hz, 1H), 4.68 (s, 2H), 4.16 (q, $J = 7.2$ Hz, 2H), 3.16 (q, $J = 7.4$ Hz, 2H), 2.36 (s, 3H), 2.25 (s, 3H), 1.27 (t, $J = 7.1$ Hz, 3H), 1.18 (t, $J = 7.4$ Hz, 3H). $^{13}$C NMR (151 MHz, $CDCl_3$) δ 168.99, 145.70, 137.34, 137.06, 133.61, 128.42, 128.39, 128.15, 124.09, 119.51, 117.93, 108.27, 107.85, 50.66, 43.29, 38.01, 15.35, 10.03, 8.74, 7.40. MS (ESI) $m/z$: 399.0$[M+H]^+$. HRMS ($ESI^+$) $m/z$ calcd for $C_{22}H_{26}N_2O_3S$ $[M+H]^+$: 399.1737; found: 399.1733.

*4.2.3.3. 4-Ethyl-N-(4-(ethylsulfonyl)benzyl)-1,2,3,4-tetrahydrocyclopenta[b]indole-7- carboxamide (**4c**).* Off white solid (40.2%); mp 162.0–164.0 °C.$^1$H NMR (400 MHz, $CD_3OD$) δ 7.96 (s, 1H), 7.87 (d, $J = 8.3$ Hz, 2H), 7.62 (d, $J = 8.4$ Hz, 3H), 7.36 (d, $J = 8.7$ Hz, 1H), 4.69 (s, 2H), 4.15 (q, $J = 7.3$ Hz, 2H), 3.18 (q, $J = 7.4$ Hz, 2H), 2.90 (t, $J = 7.1$ Hz, 2H), 2.85 (t, $J = 7.0$ Hz, 2H), 2.61–2.52 (m, 2H), 1.35 (t, $J = 7.2$ Hz, 3H), 1.19 (t, $J = 7.4$ Hz, 3H). $^{13}$C NMR (151 MHz, $CDCl_3$) δ 168.95, 147.51, 145.64, 142.25, 137.14, 128.47, 128.17, 124.41, 124.05, 119.03, 118.25, 118.25, 109.26, 50.66, 43.32, 39.68, 28.37, 25.07, 24.48, 15.57, 7.42. MS (ESI) $m/z$: 411.0$[M+H]^+$. HRMS ($ESI^+$) $m/z$ calcd for $C_{23}H_{26}N_2O_3S$ $[M+H]^+$: 411.1737; found: 411.1731.

*4.2.3.4. 1-Ethyl-N-(4-(ethylsulfonyl)benzyl)-1H-indole-5-carboxamide (**4d**).* Off white solid (89.7%); mp 111.0–113.0 °C.$^1$H NMR (400 MHz, $CDCl_3$) δ 8.17 (s, 1H), 7.72 (d, $J = 8.6$ Hz, 1H), 7.66 (d, $J = 8.1$ Hz, 2H), 7.56–7.45 (m, 1H), 7.40 (d, $J = 8.0$ Hz, 2H), 7.30 (d, $J = 8.6$ Hz, 1H), 7.14 (d, $J = 2.9$ Hz, 1H), 6.48 (d, $J = 2.4$ Hz, 1H), 4.65 (d, $J = 5.8$ Hz, 2H), 4.14 (q, $J = 7.2$ Hz, 2H), 3.01 (q, $J = 7.4$ Hz, 2H), 1.42 (t, $J = 7.2$ Hz, 3H), 1.18 (t, $J = 7.4$ Hz, 3H). $^{13}$C NMR (151 MHz, DMSO-d6) δ 167.82, 146.97, 137.41, 137.28, 129.91, 128.37, 128.04, 125.53, 120.95, 120.92, 109.78, 102.22, 49.74, 42.86, 40.95, 15.91, 7.63. MS (ESI) $m/z$: 371.0$[M+H]^+$. HRMS ($ESI^+$) $m/z$ calcd for $C_{20}H_{22}N_2O_3S$ $[M+H]^+$: 371.1424; found: 371.1423.

### 4.3. Biological assays

#### 4.3.1. RORγ FRET assay

The assays were performed in an assay buffer consisting of 50 mM NaF, 50 mM 3-(*N*-morpholino)propanesulfonic acid, pH 7.4, 0.05 mM 3-[(3-cholamidopropyl) dimethylammonio]propanesulfonate, 0.1 mg/mL bovine serum albumin, and 10 mM dithiothreitol in 384-well plates. The total volume was 25 μL/well. The europium-labeled SRC1 solution was prepared by adding an appropriate amount of biotinylated SRC and europium labeled streptavidin into assay buffer, with final concentrations of 20 and 10 nM, respectively. The allophycocyanin (APC)-labeled-LBD solution was prepared by adding an appropriate amount of biotinylated RORc-LBD and APC-labeled streptavidin at final concentrations of 20 and 10 nM, respectively. After 15 min of incubation at room temperature, a 20-fold excess of biotin was added and incubated for 10 min at room temperature to block the remaining free streptavidin. Equal volumes of europium-labeled SRC and APC-labeled RORc-LBD were then mixed with 0.1 μM surrogate agonist *N*-(2-chloro-6-fluorobenzyl)-*N*-((20-methoxy-[1,10-biphenyl]-4-yl) methyl)benzenesulfonamide and dispensed into 384-well assay plates at 25 μL volume/well. The 384-well assay plates had 100 nL of test compound in DMSO predispensed into each well. The plates were incubated for 1 h at room temperature and then read on Envision in LANCE mode configured for europeum-APC labels.

#### 4.3.2. Mouse Th17 differentiation assay

$CD4^+$ T cells were purified from mouse splenocytes using a commercial $CD4^+$ T cell negative selection kit (Invitrogen). $CD4^+$ T cells were skewed to Th17 cells by culturing cells in the presence of anti-CD3 (0.25 μg/mL, Bioxcel), anti-CD28 (1 μg/mL, Bioxcel), anti-IFN-γ (2 μg/mL, Bioxcel), anti-IL-4 (2 μg/mL, Bioxcel), TGF-β (5 ng/mL, Peprotech) and IL-6 (20 ng/mL, Peprotech) for 4 days before analysis. Compounds or DMSO control were added to the culture on day 0 of Th17 differentiation at indicated concentrations. Percentage of IL-17 production from $CD4^+$ T cells were analyzed by intracellular staining followed by flow cytometry. Dose-response curves were plotted to determine half-maximal inhibitory concentrations ($IC_{50}$) for the compounds using the GraphPad Prism 5 (GraphPad Software, San Diego CA, USA).

#### 4.3.3. Molecular docking studies

Molecular docking was carried out using Schrodinger 3.5 software package. The co-crystal structure of RORγt LBD (PDB: 4NIE) was selected and processed using the Protein Preparation Wizard including water deletion, addition of missing hydrogen atoms as well as adjustment of the tautomerization and protonation states of histidine. The compound 3D structures were subjected to energy minimization with force field (OPLS_2005) before submitting to the docking procedure. The docking grid was centered according to the ligand position, and the bounding box was set to 15 Å. This docking was performed with Glide-docking using Extra Precision (GlideXP) algorithm. The final ranking from the docking was based on the docking score, which combines the Epik state penalty with the Glide Score. High-scoring complexes were inspected visually to select the most reasonable solution.

## Acknowledgements

This work was supported by National Science Foundation of China (Grant Number: 81573276) and Shanghai Biopharmaceutical Science and Technology Supporting Plan (Grant Numbers: 15431900300 and 17431902100).

## Appendix A. Supplementary data

Supplementary data related to this article can be found at https://doi.org/10.1016/j.ejmech.2018.02.050.

## References

[1] V. Dardalhon, T. Korn, V.K. Kuchroo, A.C. Anderson, Role of Th1 and Th17 cells in organ-specific autoimmunity, J. Autoimmun. 31 (2008) 252–256.
[2] Y. Komiyama, S. Nakae, T. Matsuki, A. Nambu, H. Ishigame, S. Kakuta, K. Sudo, Y. Iwakura, IL-17 plays an important role in the development of experimental autoimmune encephalomyelitis, J. Immunol. 177 (2006) 566–573.
[3] J.S. Tzartos, M.A. Friese, M.J. Craner, J. Palace, J. Newcombe, M.M. Esiri, L. Fugger, Interleukin-17 production in central nervous system-infiltrating T cells and glial cells is associated with active disease in multiple sclerosis, Am. J. Pathol. 172 (2008) 146–155.
[4] I.I. Ivanov, B.S. McKenzie, L. Zhou, C.E. Tadokoro, A. Lepelley, J.J. Lafaille, D.J. Cua, D.R. Littman, The orphan nuclear receptor RORgammat directs the differentiation program of proinflammatory IL-17+ T helper cells, Cell 126 (2006) 1121–1133.
[5] L.A. Solt, T.P. Burris, Action of RORs and their ligands in (patho)physiology, Trends Endocrinol. Metab. 23 (2012) 619–627.
[6] N. Manel, D. Unutmaz, D.R. Littman, The differentiation of human T(H)-17 cells requires transforming growth factor-beta and induction of the nuclear receptor RORgammat, Nat. Immunol. 9 (2008) 641–649.
[7] J.R. Huh, D.R. Littman, Small molecule inhibitors of RORgammat: targeting Th17 cells and other applications, Eur. J. Immunol. 42 (2012) 2232–2237.
[8] T.P. Burris, S.A. Busby, P.R. Griffin, Targeting orphan nuclear receptors for treatment of metabolic diseases and autoimmunity, Chem. Biol. 19 (2012) 51–59.
[9] T.G.M. Dhar, Q. Zhao, D.W. Markby, Chapter twelve - targeting the nuclear hormone receptor RORγt for the treatment of autoimmune and inflammatory disorders, in: C.D. Manoj (Ed.), Annu. Rep. Med. Chem, Academic Press, 2013, pp. 169–182.
[10] S. Xiao, N. Yosef, J. Yang, Y. Wang, L. Zhou, C. Zhu, C. Wu, E. Baloglu, D. Schmidt, R. Ramesh, M. Lobera, M.S. Sundrud, P.Y. Tsai, Z. Xiang, J. Wang, Y. Xu, X. Lin, K. Kretschmer, P.B. Rahl, R.A. Young, Z. Zhong, D.A. Hafler, A. Regev, S. Ghosh, A. Marson, V.K. Kuchroo, Small-molecule RORgammat antagonists inhibit T helper 17 cell transcriptional network by divergent mechanisms, Immunity 40 (2014) 477–489.
[11] J.S. Lee, D.J. Cua, The emerging landscape of RORgammat biology, Immunity 40

(2014) 451–452.
[12] J. Yang, M.S. Sundrud, J. Skepner, T. Yamagata, Targeting Th17 cells in autoimmune diseases, Trends Pharmacol. Sci. 35 (2014) 493–500.
[13] F. Isono, S. Fujita-Sato, S. Ito, Inhibiting RORgammat/Th17 axis for autoimmune disorders, Drug Discov. Today 19 (2014) 1205–1211.
[14] C. Dong, Targeting Th17 cells in immune diseases, Cell Res. 24 (2014) 901–903.
[15] J.R. Huh, M.W. Leung, P. Huang, D.A. Ryan, M.R. Krout, R.R. Malapaka, J. Chow, N. Manel, M. Ciofani, S.V. Kim, A. Cuesta, F.R. Santori, J.J. Lafaille, H.E. Xu, D.Y. Gin, F. Rastinejad, D.R. Littman, Digoxin and its derivatives suppress TH17 cell differentiation by antagonizing RORgammat activity, Nature 472 (2011) 486–490.
[16] L.A. Solt, N. Kumar, P. Nuhant, Y. Wang, J.L. Lauer, J. Liu, M.A. Istrate, T.M. Kamenecka, W.R. Roush, D. Vidovic, S.C. Schurer, J. Xu, G. Wagoner, P.D. Drew, P.R. Griffin, T.P. Burris, Suppression of TH17 differentiation and autoimmunity by a synthetic ROR ligand, Nature 472 (2011) 491–494.
[17] T. Xu, X. Wang, B. Zhong, R.I. Nurieva, S. Ding, C. Dong, Ursolic acid suppresses interleukin-17 (IL-17) production by selectively antagonizing the function of RORgamma t protein, J. Biol. Chem. 286 (2011) 22707–22710.
[18] B.P. Fauber, S. Magnuson, Modulators of the nuclear receptor retinoic acid receptor-related orphan receptor-gamma (RORgamma or RORc), J. Med. Chem. 57 (2014) 5871–5892.
[19] Y. Zhang, X.Y. Luo, D.H. Wu, Y. Xu, ROR nuclear receptors: structures, related diseases, and drug discovery, Acta Pharmacol. Sin. 36 (2015) 71–87.
[20] P. Cyr, S.M. Bronner, J.J. Crawford, Recent progress on nuclear receptor RORc modulators, Bioorg. Med. Chem. Lett 26 (2016) 4387–4393.
[21] S.M. Bronner, J.R. Zbieg, J.J. Crawford, RORγ antagonists and inverse agonists: a patent review, Expert Opin. Ther. Pat. 27 (2017) 101–112.
[22] Y. Wang, W. Cai, G. Zhang, T. Yang, Q. Liu, Y. Cheng, L. Zhou, Y. Ma, Z. Cheng, S. Lu, Y.G. Zhao, W. Zhang, Z. Xiang, S. Wang, L. Yang, Q. Wu, L.A. Orband-Miller, Y. Xu, J. Zhang, R. Gao, M. Huxdorf, J.N. Xiang, Z. Zhong, J.D. Elliott, S. Leung, X. Lin, Discovery of novel N-(5-(arylcarbonyl)thiazol-2-yl)amides and N-(5-(arylcarbonyl)thiophen-2-yl)amides as potent RORgammat inhibitors, Bioorg. Med. Chem. 22 (2014) 692–702.
[23] Y. Wang, T. Yang, Q. Liu, Y. Ma, L. Yang, L. Zhou, Z. Xiang, Z. Cheng, S. Lu, L.A. Orband-Miller, W. Zhang, Q. Wu, K. Zhang, Y. Li, J.N. Xiang, J.D. Elliott, S. Leung, F. Ren, X. Lin, Discovery of N-(4-aryl-5-aryloxy-thiazol-2-yl)-amides as potent RORgammat inverse agonists, Bioorg. Med. Chem. 23 (2015) 5293–5302.
[24] T. Yang, Q. Liu, Y. Cheng, W. Cai, Y. Ma, L. Yang, Q. Wu, L.A. Orband-Miller, L. Zhou, Z. Xiang, M. Huxdorf, W. Zhang, J. Zhang, J.N. Xiang, S. Leung, Y. Qiu, Z. Zhong, J.D. Elliott, X. Lin, Y. Wang, Discovery of tertiary amine and indole derivatives as potent RORgammat inverse agonists, ACS Med. Chem. Lett. 5 (2014) 65–68.
[25] Y. Wang, W. Cai, Y. Cheng, T. Yang, Q. Liu, G. Zhang, Q. Meng, F. Han, Y. Huang, L. Zhou, Z. Xiang, Y.G. Zhao, Y. Xu, Z. Cheng, S. Lu, Q. Wu, J.N. Xiang, J.D. Elliott, S. Leung, F. Ren, X. Lin, Discovery of biaryl amides as potent, orally bioavailable, and CNS penetrant RORgammat inhibitors, ACS Med. Chem. Lett. 6 (2015) 787–792.
[26] Y. Wang, W. Cai, Q. Liu, Q. Meng, Y. Cheng, T. Yang, G. Zhang, J. Xiang, C. Wu, in: Preparation of N-substituted 2-[4-(ethylsulfonyl)phenyl]acetamides as Retinoid-related Orphan Receptor Gamma Modulators, Glaxo Group Limited, UK, 2013, p. 260. Application: WO2013/029338A1.
[27] D.R. Withers, M.R. Hepworth, X. Wang, E.C. Mackley, E.E. Halford, E.E. Dutton, C.L. Marriott, V. Brucklacher-Waldert, M. Veldhoen, J. Kelsen, R.N. Baldassano, G.F. Sonnenberg, Transient inhibition of ROR-γt therapeutically limits intestinal inflammation by reducing TH17 cells and preserving group 3 innate lymphoid cells, Nat.Med. 22 (2016) 319–323.
[28] C.A. Lipinski, F. Lombardo, B.W. Dominy, P.J. Feeney, Experimental and computational approaches to estimate solubility and permeability in drug discovery and development settings, Adv. Drug Deliv. Rev. 46 (2001) 3–26.
[29] S. Yamamoto, J. Shirai, Y. Fukase, Y. Tomata, A. Sato, A. Ochida, K. Yonemori, H. Nakagawa, in: Preparation of Indole and Carbazole Derivatives as Inhibitors of Retinoid-related Orphan Receptor γt (RORγt), Takeda Pharmaceutical Company Limited, Japan, 2013, p. 122. Application: WO2013/042782.
[30] Y. Wang, W. Cai, T. Tang, Q. Liu, T. Yang, L. Yang, Y. Ma, G. Zhang, Y. Huang, X. Song, L.A. Orband-Miller, Q. Wu, L. Zhou, Z. Xiang, J.-N. Xiang, S. Leung, L. Shao, X. Lin, M. Lobera, F. Ren, From RORγt agonist to two types of RORγt inverse agonists, ACS Med. Chem. Lett. 9 (2018) 120–124.